

https://dspace.org/

The use of South African coal fly ash (CFA) as an additive to oil well cement during cementing operation

Kaduku, Tendai

2016-03-17
http://hdl.handle.net/10539/20109

Downloaded from a DSpace repository. https://dspace.org/

Characterization and Performance Evaluation of Sodium Silicate derived from South African Coal Fly Coal as an Extender in Oil Well Cementing

T. Kaduku , M.O. Daramola*, F.O. Obazu, S.E. Iyuke

School of Chemical and Metallurgical Engineering, Faculty of Engineering and the Built Environment, University of Witwatersrand, Johannesburg, South Africa

*Corresponding author: Email: michael.daramola@wits.ac.za; +27 117 177 536

Abstract

About 25 million tons of coal fly ash (CFA) is produced annually in South Africa and its disposal constitutes a huge environmental problem at the moment. Although the use of CFA in oil well cement (OWC) has been reported, but composition of the CFA differs from country to country and this could affect its suitability as additive in OWC operation. In addition, use of raw CFA results in slower strength gain and longer setting times, thereby resulting in low early-age strength and delays in the well completion process. In this work, beneficiation of South African CFA in OWC operation is reported. Silica (SiO_2) was extracted from the CFA and used to synthesize sodium silicate (CFA-Na_2SiO_3), typical OWC slurry extender. Physicochemical properties of the CFA-Na_2SiO_3 were compared to those of a commercial sodium silicate (com-Na_2SiO_3) using SEM, XRD and FTIR. OWC slurries with varying compositions of cement, distilled water and 2 % $CaCl_2$ by-weight-of-water (BWOW) were prepared and extended using the CFA-Na_2SiO_3 and the com-Na_2SiO_3 at compositions ranging from 0.25-2.5 % by-weight-of-cement (BWOC). Rheological properties of the slurries were evaluated using API procedures and compared. The physico-chemical properties of the CFA-Na_2SiO_3 are consistent with that of com-Na_2SiO_3, indicating the purity of the CFA-Na_2SiO_3. Comparative study between the OWC slurries indicate that the slurries extended with CFA-Na_2SiO_3 have slightly lower densities, lower viscosities and higher compressive strength compared to those extended with com-Na_2SiO_3. This indicates that CFA-Na_2SiO_3 slurries would be easier to pump and preferable where early strength development is critical. This report opens up a way for the beneficiation of South African CFA in the petroleum, oil and gas industry.

Keywords: Oil well cementing, coal fly ash, sodium silicate, compressive strength

Introduction

During the oil and gas well cementing process, some wells often possess lost circulation zones, and therefore prone to formation breakage. Often, low density slurries are required to overcome these problems, and extenders, which help to reduce the weight of the slurry, are utilized (Salim and Amani 2013; Ahmaruzzaman 2010; Shahriar 2011). The commonly used extenders are water extenders such as bentonite and sodium silicate, which allow excessive addition of water to the slurry and low density aggregates such as microspheres and pozzolans, which have densities that are lower than that of Portland cement (3.15 $g.cm^{-3}$) (Nelson et al. 1990). These extenders reduce the density of the slurry, resulting in a reduction of the hydrostatic pressure during cementing (Nelson et al. 1990). Extenders also increase slurry yield by replacing a substantial amount of cement required to complete a given task.

One of the most commonly used water extenders is Na_2SiO_3 and reported to be about five times more effective as an extender when compared to bentonite (Nelson et al. 1990). Unlike pozzolanic extenders such as fly ash, Na_2SiO_3 is highly reactive with oil well cement (Joel and Ujile 2009). Na_2SiO_3 reacts with the Ca^{2+} ions from the lime in the OWC or calcium chloride to produce additional calcium-silica-hydrate (C-S-H) gel (Nelson et al. 1990). The gel structure provides sufficient viscosity to allow the use of large quantities of mix water without excessive free water separation (Nelson et al. 1990). The further C-S-H formation also results in a reduction in thickening time, and hence the accelerating effect of Na_2SiO_3 (Joel and Ujile 2009). The advantages of Na_2SiO_3 as an extender include low concentration of use and high yield as compared to other extenders such as bentonite and coal fly ash (Joel and Ujile 2009). Whilst fly ash is added in concentrations of up to 50 % by-weight-of-cement (BWOC) and bentonite up to 20 % BWOC, Na_2SiO_3 ranges from 0.2% to 3.0% BWOC (Nelson et al. 1990). The accelerating effect of Na_2SiO_3, however, limits its application at lower temperatures, typically less than 52 °C bottom hole circulating temperature (BHCT) (Nelson et al. 1990; Joel and Ujile 2009).However, it can be used at higher temperatures with the addition of a retarder, although its effectiveness as an extender is reduced because of the inhibition of C-S-H formation (Nelson *et al.*, 1990; Joel and Ujile, 2009).

At industrial scale, commercial sodium silicate is traditionally manufactured through calcining sodium carbonate (Na_2CO_3) and SiO_2 at temperature ranges of 1400-1500 °C in furnaces (Folleto *et al*., 2006). Although the raw materials are cheap, the process is not cost-effective due to its high energy consumption and maintenance cost (Folleto *et al.*, 2006). The process also emits dust, nitrogen and sulphur oxides, contributing therefore to air pollution. Alternatively, Na_2SiO_3 can be produced through the reaction of SiO_2 with NaOH solution in an autoclave, at high temperature and pressure (McDaniel *et al*., 1961). In light of the information at hand, it is necessary to carry out an investigation on alternative methods, which are less energy intensive, for producing Na_2SiO_3 for use as an additive to OWC.

Coal fly ash (CFA) is an inorganic powder that is produced during the combustion of coal (Ahmaruzzaman, 2010). Several studies have been carried out and reported on the beneficiation of CFA (Iyer and Scott, 2001; Ahmaruzzaman, 2010, Taylor1990), Kamarudin *et al.*,2009; Park *et al.*, 2012). Beneficiation of fly ash from other materials such as rice husks, bagasse and corn cobs has also been reported (Aigbodion *et al.*, 2010; Foleto *et al*., 2006; Okoronkwo *et al.*, 2013). Even, the use of CFA in oil well cement (OWC) has been reported (Shahriar, 2011), but composition of the CFA differs from country to country and this could affect its suitability as additive in OWC operation. Furthermore, the use of raw CFA results in slower strength gain and longer setting times, thereby resulting in low early-age strength and delays in the well completion process (Bazzar *et al.*, 2013). In South Africa, about 25 million tons of coal fly ash (CFA) is produced annually and its disposal constitutes a huge environmental problem at the moment. In this study, SiO_2 was extracted from CFA and used as starting material to synthesize Na_2SiO_3. The performance of the synthesized CFA-derived sodium silicate (CFA-Na_2SiO_3) as an OWC extender was evaluated and compared with that of the commercial sodium silicate (com-Na_2SiO_3).

Materials and Methods

Materials

Class G cement (Dyckerhoff), CFA (Power Station-X in South Africa), demineralized water (prepared in-house), all chemicals: hydrochloric acid solution (37 %), sodium hydroxide pellets (98 % purity), calcium chloride (99.99 % purity) and commercial sodium metasilicate (95 %) were purchased from Sigma Aldrich and used as delivered without any modification or purification.

Methods

CFA sample preparation and characterization

Small quantities of CFA were scooped randomly from different points and then mixed together to make the representative sample. The CFA samples were characterized using X-ray Diffraction (XRD: Brucker D2 X-ray Diffraction machine), X-ray Fluorescence (XRF: PANalytical AXIOS X-Ray Fluorescence Spectrometer), Scanning Electron Microscopy (SEM: ZEISS Sigma VP Field Emission-SEM), and Thermogravimetric analysis (TGA: TGA DSC STA 600 with Pyris software). The pH of CFA (dissolved in water) was measured using a Metrohm 744 pH meter and the particle size distribution of the CFA was obtained using a Malvern Mastersizer 2000.

Extraction of SiO_2 and preparation of Na_2SiO_3 from CFA

The metal oxides such as Al_2O_3 and CaO were removed from CFA through acid refluxing using 3 M HCl at 100 °C for 6 hours as described elsewhere (Tang *et al.,* 2012). The solid product, SiO_2, was filtered out and purified through successive demineralized water washing. The wet SiO_2 was dried in an oven at 200 °C for 2 hours to obtain an amorphous silica powder which was then analysed using SEM-EDX, XRD and Fourier Transform Infrared spectroscopy (FTIR: Brüker Tensor 27 Fourier Transform Infrared spectrometer). 60 g of the amorphous silica was reacted with 80 g sodium hydroxide pellets in 100 ml distilled water in a Pyrex flat bottomed flask at 80 °C and atmospheric pressure to produce colourless viscous solution. The solution was then poured into a crucible and calcined at 300°C for 3 hours to produce a white solid (CFA-Na_2SiO_3) which was crushed into a powder using a mortar and pestle. The product was then subjected to SEM-EDX, XRD and FTIR analyses.

Preparation and characterization of cement slurries

Slurries containing varying amounts of cement, distilled water, 2 % calcium chloride ($CaCl_2$) by-weight-of-water (BWOW), com-Na_2SiO_3 and CFA-Na_2SiO_3 were prepared and their performances were evaluated on density, rheology and thickening time. A Chandler Ametek Constant Speed Mixer (Model 30-60) was used for mixing and the slurries were pre-conditioned using a Chandler Ametek Atmospheric Consistometer (Model 1200) prior to the rheology tests. The rheology tests were done using a Chandler Ametek Automated Viscometer (Model 3530) and a Chandler Ametek Pressurized Mud Balance was used to determine the density of the slurries. A Chandler Ametek Twin Cell Ultra Sonic Cement Analyzer (UCA) (Model 4262) was used to determine the development of compressive strength of the slurries. All the tests on the cement slurries were carried out according to the specification for materials and testing for Well Cements (API 1990).

Results and Discussions

CFA sample preparation and characterization

Figure 1 shows the XRD patterns for the CFA. The patterns show that the dominant phases are mullite Al(Al1.272Si0.728O4.864) and quartz alpha (SiO_2). Small quantities of magnesium oxide (MgO_4), lime (CaO) and iron oxide (epsilon-Fe_2O_3) were also identified. The same phases were identified in previously studied South African CFAs (*Ayanda et al.,* 2012; Mainganye *et al.,* 2013; Ikotun *et al.,* 2014). Better understanding of the quantities of these phases was obtained with XRF analysis. Table 1 shows the XRF results of the CFA from Power Station X compared with reports from literature (Ayanda *et al.,* 2012; Mainganye *et al.,* 2013). The analysis showed that the major components of the CFA from Power Station X are silica, alumina, iron oxide, calcium oxide and

carbon (inferred from the Loss on Ignition (LOI) test). The results showed that CFA from Power Station X is of class F (ASTM C618, 2012) and the order of the metal oxides decreased in the order SiO_2> Al_2O_3> Fe_2O_3> CaO> MgO> K_2O> Na_2O> TiO_2. This order is consistent with previous reports on South African CFA (Ayanda *et al.*, 2012; Mainganye *et al.*, 2013; Ikotun *et al.*, 2014). Interestingly, the CFA contained about 58 % SiO_2, the desired component for the synthesis of Na_2SiO_3.

Figure 1. XRD Diffractogram for two samples of CFA.

Table 1. XRF Results for Power Station X CFA (majors). Also included are XRF results for South African CFAs (Mainganye *et al.*, 2013and Ayanda *et al.*, 2012)

The morphology of the CFA is depicted in the SEM micrograph in Figure 2. The shapes of the CFA particles are determined by their exposure conditions (time and temperature) in the combustion chamber (Fisher *et al.*, 1978). As seen in Figure 2, most of the particles are spherical, especially in the finer fractions. A similar observation has been reported for the South African CFA (Ayanda *et al.*, 2012; Mainganye *et al.*, 2013). The particles are a mixture of opaque and non-opaque spheres. The opaque spheres are predominantly iron oxides and some silicates whilst the non-opaque spheres are mainly silicates (Fisher *et al.*, 1978). Previous studies have shown that fly ash is made up of, in some cases, smaller particles which are attached to the surface of larger particles, hollow spheres (cenospheres), and some spheres containing other spheres (plerospheres) (Mainganye *et al.*, 2013). In addition, the SEM micrograph shows the presence of some non-spherical particles. These amorphous particles which are non-spherical mainly arise from incomplete combustion of coal components due to less exposure to high temperatures (Fisher *et al.*, 1978). Furthermore, the TGA conducted on the CFA shows that the CFA contains about 0.2% moisture, 1.6% volatile matter and 1.7% fixed carbon. The particle size analysis shows that the particle size of CFA ranges from 0.32-112 μm. The results are in agreement with previous studies as well (Ayanda *et al.*, 2012 ; Ikotun *et al.*, 2014). A rise in pH from 7 to 10.7 was observed when the CFA was mixed with de-ionized water over a period of 5 hours. The increase in the pH could be attributed to the dissolution of compounds such as CaO in the CFA. This observation is in good agreement with previous report (Ayanda *et al.*, 2012).

Figure2. SEM micrograph of the South African CFA

Extraction of SiO_2 and preparation of Na_2SiO_3 from CFA and characterization

Morphologies of the extracted SiO_2, synthesized CFA-Na_2SiO_3 and com-Na_2SiO_3 were checked with SEM. Figure 3 shows the SEM images of the extracted SiO_2. Similar images for precipitated SiO_2 have been reported in literature (Music *et al.*, 2011). The elemental compositions obtained using energy disperse X-ray spectroscopy (EDS) showed Si and O, indicating the presence of SiO_2. The XRD pattern in Figure 4 shows the characteristic slope and pattern for amorphous SiO_2. The pattern is a broad band with a peak which indicates that the substance is amorphous and contains pure SiO_2 (Saikia *et al.*, 2008; *Essien et al.*, 2011, Music *et al.*, 2011; Okoronwo *et al.*, 2013). Similar patterns for amorphous silica have been recorded in literature (Saikia *et al.*, 2008; Okoronwo *et al.*, 2013). The two sharp peaks on the pattern are due to the presence of quartz, corroborating the results obtained from EDS. The FTIR spectrum of the SiO_2 is depicted in Figure 5. The bands of absorption at 1199 cm^{-1}, 964 cm^{-1} and 682 cm^{-1} can be attributed to the absorption peaks characteristic of SiO_2 (Ying-Mei *et al.*, 2010). Absorption peak at 1199 cm^{-1} corresponds to the asymmetrical stretching vibration of Si – O (Ying-Mei *et al.*, 2010). In addition, absorption peaks at 964 cm^{-1} and 682 cm^{-1} correspond to the symmetrical stretching vibrations of Si – O groups on the surface of the amorphous solid (Ying-Mei *et al.*, 2010; Essien *et al.*, 2011). The stretch between 1500 cm^{-1} and 2000 cm^{-1} can be attributed to the presence of the Si–OH and bending vibration absorption of the O–H bond of physically adsorbed water respectively (Music *et al.*, 2011).

Figure 3. SEM micrograph for amorphous silica extracted from the South African CFA

Figure 4. XRD Spectra for the amorphous silica extracted from the South Africa CFA

Figure 5. FTIR Spectra for the amorphous silica extracted from the South African CFA

The XRD patterns for CFA-Na_2SiO_3 and com-Na_2SiO_3 are shown in Figure 6. The two patterns are similar, although a little difference in the intensities of some of the peaks was observed. Curve fitting showed that there is a slight shift in the peaks of CFA-Na_2SiO_3. The shift in the peaks could be attributed to the small quantity of the sample used in the analysis. Figure 7 depicts the SEM images for CFA-Na_2SiO_3 and com- Na_2SiO_3. The morphology of the CFA-Na_2SiO_3 is totally different from that of com-Na_2SiO_3. However, the EDS showed the same elemental components with different compositions. Figure 8 shows the IR spectra for the commercial sodium silicate and CFA sodium silicate. The FTIR analysis of the two samples indicates that there is no observable chemical difference in the samples. FTIR of both samples show absorption bands at 2340 cm^{-1}, 1160 cm^{-1}, 1125 cm^{-1}, 980 cm^{-1}, and 715 cm^{-1} that characterize the presence of sodium metasilicate (Miller and Wilkins, 1952). The stretch between 1500 cm^{-1} and 2000 cm^{-1} could be attributed to the presence of the Si–OH and bending vibration absorption of the O–H bond (Ying-Mei *et al.*, 2010).

Figure 6. XRD diffractograms for commercial sodium silicate (com-Na_2SiO_3) and CFA sodium silicate (CFA-Na_2SiO_3) .

Figure 7. SEM micrographs for commercial sodium silicate (com-Na_2SiO_3) and CFA sodium silicate (CFA-Na_2SiO_3)

Figure 8. FTIR Spectra for commercial sodium silicate (com-Na_2SiO_3) and CFA sodium silicate (CFA-Na_2SiO_3)

Preparation and characterization of cement slurries

The compositions and the densities of the slurries prepared using CFA-Na_2SiO_3 and com-Na_2SiO_3 as additives are shown in Table 2. The slurries had similar densities with slight differences as the amount of additive added increases. Some of the slurries containing CFA-Na_2SiO_3 had slightly lower densities compared to the slurries containing com-Na_2SiO_3. There was a 0.02 % difference in the densities of the slurries containing 2 % additive. The difference may be due to that slurries prepared using CFA-Na_2SiO_3 had a lot of froth. Rheology of slurries prepared using CFA-Na_2SiO_3 and com-Na_2SiO_3 as additives are shown in Tables 3 and 4, respectively. The slurries prepared using both additives exhibited good rheology with plastic viscosities (P_v) between 3.75 and 18.75 cp and yield points (Y_p) between 13.5 and 61.75 lb/100ft^2. The slurries containing com-Na_2SiO_3 generally had higher rheological values compared to those prepared using the CFA-Na_2SiO_3. At 60 rpm the viscosity of the slurry containing 1% com-Na_2SiO_3 was 45 cp whilst that for the CFA-Na_2SiO_3 slurry was 26 cp. The slurries prepared using CFA-Na_2SiO_3 were less viscous and this can be attributed to the presence of froth.

Table 2. Compositions and densities of the slurries

Table 3. Rheological properties of the slurries with com-Na_2SiO_3.

Table 4. Rheological properties of the slurries with CFA-Na_2SiO_3.

Table 5. UCA results for the slurries with com-Na_2SiO_3

Table 6. UCA results for the slurries with CFA-Na_2SiO_3.

Tables 5 and 6 show the compressive strength results for slurries containing com-Na_2SiO_3 and CFA-Na_2SiO_3 ,respectively. As expected, there was a decrease in compressive strength for all slurries as the amount of water added increased. Figures 9-11 show that the slurries containing CFA-Na_2SiO_3 had higher compressive strength than those containing com-Na_2SiO_3 at 8 hours, 12 hours and 24 hours , respectively. From Tables 5 and 6 , it can be observed that the CFA-Na_2SiO_3 slurries gained the compressive strength of 50 psi earlier than the Na_2SiO_3 slurries. This is the minimum strength required to hold the casing in position. The same observation was obtained for slurries which managed to gain compressive strength of 500 psi within the first 24 hours. 500 psi is the sufficient strength required to hold the casing where further drilling or perforation of the casing need to be done.

Figure 9. Compressive strength results at 8 hours.

Figure 10. Compressive strength results at 12 hours.

Figure 11. Compressive strength results at 24 hours.

Conclusion

Results of this study indicate that the South African CFA used in this study belongs to Class F of CFA and contains 58 % amorphous SiO_2. The physico-chemical properties of the synthesized Na_2SiO_3 are consistent with that of the commercial Na_2SiO_3, indicating the purity of the as-prepared Na_2SiO_3 from the CFA. In addition, the synthesis protocol, which was at a mild temperature, confirms the energy efficiency of the method used. Characterization of the cement slurries prepared with CFA-Na_2SiO_3 show better performance than that with com-Na_2SiO_3. The rheology results showed that CFA-Na_2SiO_3 made slurries that are less viscous than the slurries made with com-Na_2SiO_3, making slurries with CFA- Na_2SiO_3 less difficult to pump. Comparing the UCA results showed that the slurries containing CFA Na_2SiO_3 have higher compressive strength than those containing com-Na_2SiO_3. This means that the WOC is reduced when CFA-Na_2SiO_3 is used as an additive and as a result the job can be completed in less time that it is required. Where early strength development is critical, CFA-Na_2SiO_3 slurries are therefore preferred. This report opens up a way for the beneficiation of South African CFA in the petroleum, oil and gas industry.

Acknowledgements

The authors hereby acknowledge the financial support from Chemical Industries Education and Training Authorities (CHIETA) South Africa and Baker Hughes South Africa (Mossel Bay) for availing their cement testing laboratory facility.

References

Ahmaruzzaman, M. 2010. A review on the utilization of fly ash, *Progress in Energy and Combustion Science*, vol. 36, no. 1, pp. 327-363.

Aigbodion, V. S., Hassan, S. B., Ause, T. and Nyior, G. B. 2010. Potential utilization of solid waste (bagasse ash), *Journal of Minerals & Materials Characterization & Engineering*, vol. 9, no. 1, pp. 67-77.

American Petroleum Institute Specification 10A (2002). Specifications for Cementing and Materials for Well Cementing, *ANSI/API 10A/ISO 10426-1*-2001.

ASTMC618. 2012. Standard specification for coal fly ash and raw or calcined natural Pozzolan for use in concrete.

Ayanda, O. S., Fatoki, O. S., Adekola, F. A. and Ximba B. J. 2012. Characterization of fly ash generated from Matla Power Station in Mpumalanga, South Africa, *E-Journal of Chemistry*, vol. 9, no. 4, pp. 1788 -1795.

Essien, E. R., Olaniyi O. A., Adams L. A. and Shaibu R. O. 2011. Highly porous silica network prepared from sodium metasilicate, *Journal of Metals, Materials and Minerals*, vol. 21, no. 2, pp. 7-12.

Fisher, G. L., Prentice, B. A., Silberman, D., Ondov, J. M., Biermann, A. H., Ragaini, R. C. and McFarland A. R. 1978. Physical and morphological studies of size- classified coal fly ash, *The American Chemical Society*, vol. 12, no. 4, pp. 477- 451.

Foletto, E. L., Gratieri, E., Hadlich de Oliveira, L. and Jahn S. L. 2006. Conversion of Rice Hull Ash into Soluble Sodium Silicate, *Materials Research*, vol. 9, no. 3, pp. 335-338.

Ikotun, B. D., Mishra, S. and Fanourakis G. C.2014. Structural Characterization of Four South African Fly Ashes and Their Structural Changes with β-Cyclodextrin, *Particulate Science and Technology: An International Journal*, vol. 32, no. 4, pp. 360-365.

Iyer, R. S. and Scott, J. A. 2001. Power station fly ash - A review of value-added utilization outside of the construction industry, *Resources, Conservation and Recycling*, vol. 31, pp. 217–228.

300 Joel, O. F. and Ujile, A. A. 2009. Performance evaluation of Low Density Bentonite and Econolite
301 Cement, Nigeria, *International Journal of Natural and Applied Science*, vol. 5, no. 4, pp. 322-
302 328.
303 Kamarudin, R. A., Matlob, A. S., Jubri, Z. and Ramli Z. 2009. Proceedings of ICEE 2009 3rd
304 International Conference on Energy and Environment. Malacca, Malaysia.
305 Lea, F.M. 1971. The Chemistry of Cement and Concrete, Chemical Publishing Company Inc. New
306 York, USA.
307 Mainganye, D., Ojumu, T. V. and Petrik, L. (2013). Synthesis of zeolites Na-P1 from South African
308 coal fly ash: Effect of impeller design and agitation, *Materials*, vol. 6, pp. 2074- 2089.
309 McDaniel, G. R. 1961. Wet Production of Silicates. United States Patent Office. Patent no.
310 US2983423.
311 Miller, F. A. and Wilkins, C. H. 1952. Infrared spectra and characteristic frequencies of inorganic
312 ions: Their use in qualitative analysis, *Analytical Chemistry*, vol. 24, no. 8, pp. 1253- 1294.
313 Music, S., Vincekovic, N. F. and Sekovanic, L. 2011. Precipitation of amorphous SiO_2 particles and
314 their properties, *Brazilian Journal of Chemical Engineering*, vol. 28, no. 1, pp. 89- 94.
315 Nelson, E.B. and Guillot, D. 1990, *Well Cementing*, 2nd (eds)., Schlumberger, Texas
316 Nelson, E.B., Baret, J.F. and Michaux, M.1990, *Well Cementing: Cement Additives and Mechanisms*
317 *of Action*, Elsevier B. V, USA.
318 Okoronkwo, E. A., Imoisili, P. E. and Olusunle, S. O. O. 2013. Extraction and characterization of
319 Amorphous Silica from Corn Cob Ash by Sol-Gel Method, *Chemistry and Materials Research*,
320 vol. 3, no. 4, pp. 68-72.
321 Park, J., Han, Y. and Kim H. 2012. Formation of Mesoporous Materials from Silica Dissolved in
322 Various NaOH Concentrations: Effect of pH and Ionic Strength, *Journal of Nanomaterials*, vol.
323 528174, pp. 1-10.
324 Saikia, B. J., Parthasarathy, G., Sarmah ,N. C. and Baruah G. D. 2008. Fourier transform infrared
325 spectroscopic characterization of naturally occurring glassy fulgurites, *Bulletin of Material*
326 *Science*, vol. 31, no. 2, pp. 155-158.

Salim, P. and Amani, M. 2013. Special Considerations in Cementing High Pressure High Temperature Wells, *International Journal of Engineering and Applied Sciences*, vol.1, no. 4, pp. 1-24.

Shahriar, A.2011. Investigation on Rheology of Oil Well Cement Slurries, *PhD Thesis*, The University of Western Ontario London. Canada.

Tang, C., Thawornsak, N., Samrankrang, S., Jullaphan, O. and Chareonpanich M. 2012. Creating High-Value Eco-Friendly Materials from Industrial Coal Combustion Ash, in proceedings of the EUROCOALASH 2012 Conference, Thessaloniki Greece.

Taylor, H. F. W. 1990. *Cement Chemistry*. Academic Press. London

Ying-Mei, X., Ji, Q., De-Min, H., Dong-Mei, W., Hui-Ying, C., Jun, G. and Qiu-Min, Z. 2010. Preparation of amorphous silica from oil shale residue and surface modification by silane coupling agent, *Oil Shale*, vol. 27, no. 1, pp. 37- 48.

Figure Captions

Figure 1. XRD Diffractogram for two samples of CFA.

Figure2. SEM micrograph of the South African CFA

Figure 3. SEM micrograph for amorphous silica extracted from the South African CFA

Figure 4. XRD Spectra for the amorphous silica extracted from the South Africa CFA

Figure 5. FTIR Spectra for the amorphous silica extracted from the South African CFA

Figure 6. XRD diffractograms for commercial sodium silicate (B: com-Na_2SiO_3) and CFA sodium silicate (A: CFA-Na_2SiO_3).

Figure 7. SEM micrographs for commercial com-Na_2SiO_3 (left) and CFA-Na_2SiO_3 (right)

Figure 8. FTIR Spectra for commercial sodium silicate (com-Na_2SiO_3) and CFA sodium silicate (CFA-Na_2SiO_3)

Figure 9. Compressive strength results at 8 hours.

Figure 10. Compressive strength results at 12 hours.

Figure 11. Compressive strength results at 24 hours.

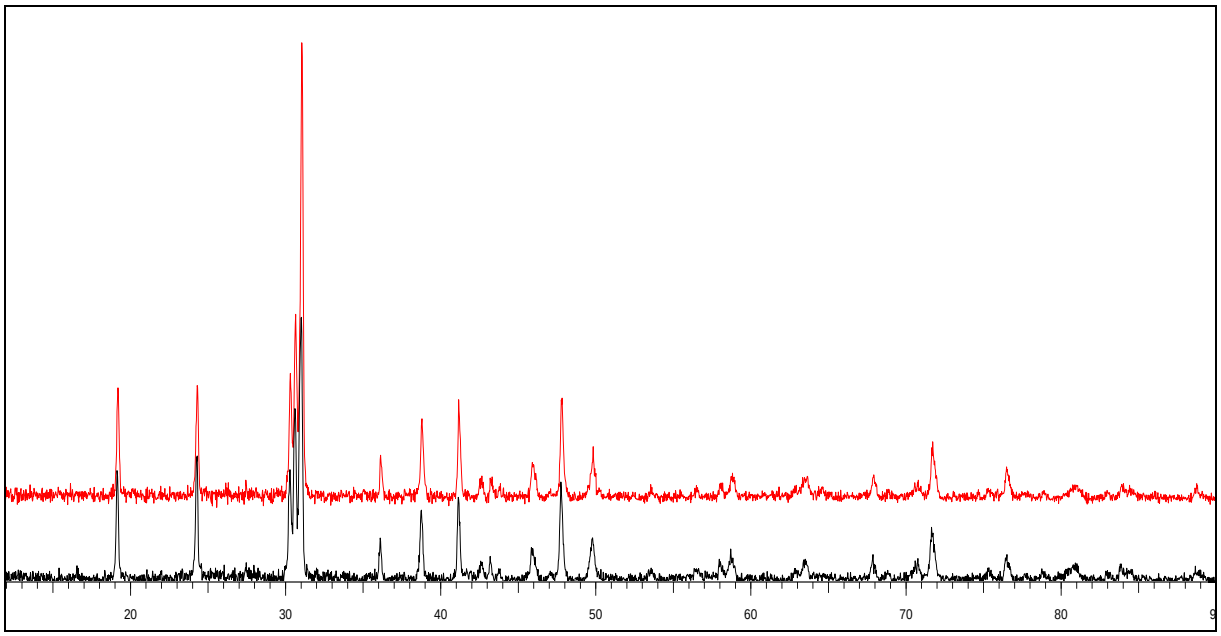


Figure 1

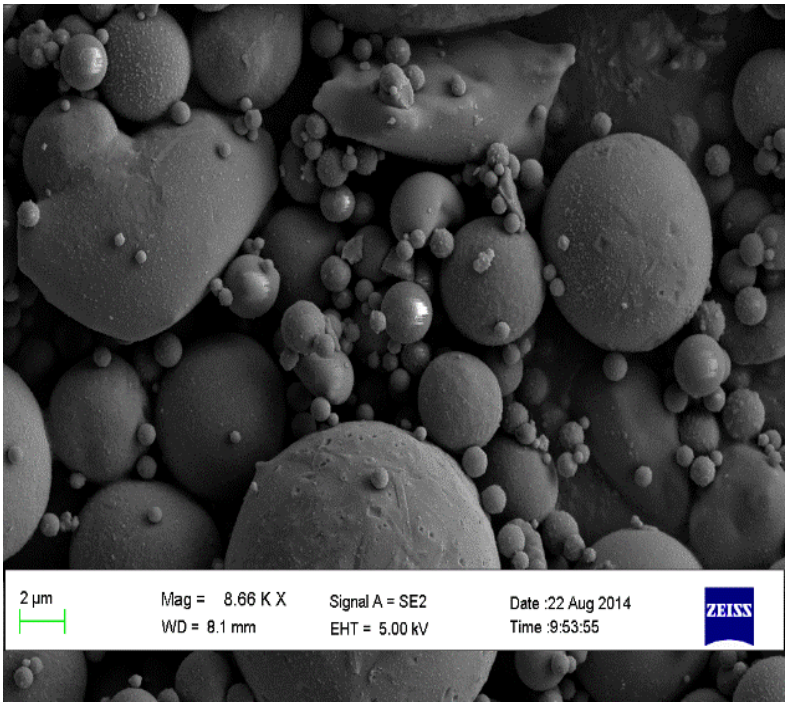

2 µm
Mag = 8.66 K X
WD = 8.1 mm
Signal A = SE2
EHT = 5.00 kV
Date :22 Aug 2014
Time :9:53:55
ZEISS

Figure 2

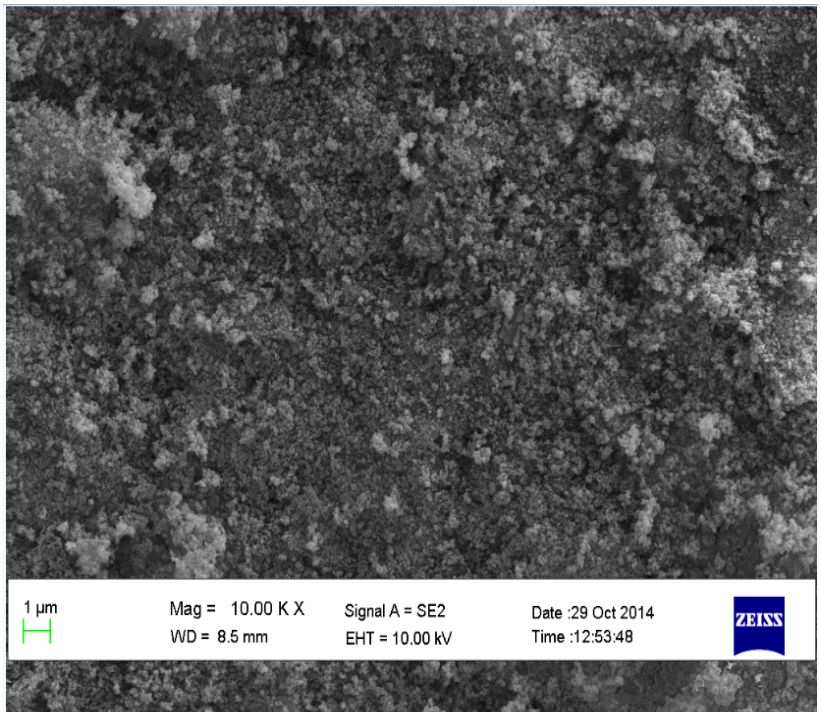

1 µm
Mag = 10.00 K X
WD = 8.5 mm
Signal A = SE2
EHT = 10.00 kV
Date :29 Oct 2014
Time :12:53:48
ZEISS

Figure 3

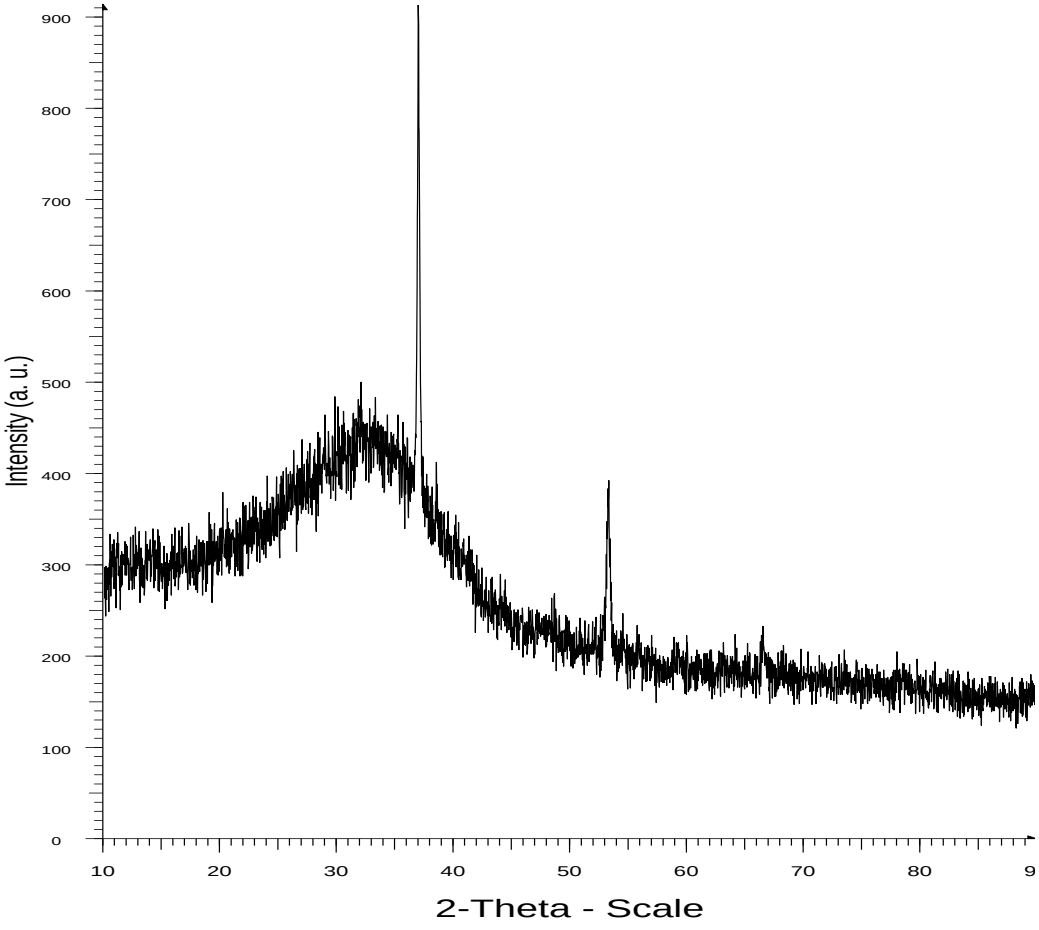

Intensity (a. u.)
900
800
700
600
500
400
300
200
100
0
10
20
30
40
50
60
70
80
9
2-Theta - Scale

Figure 4.

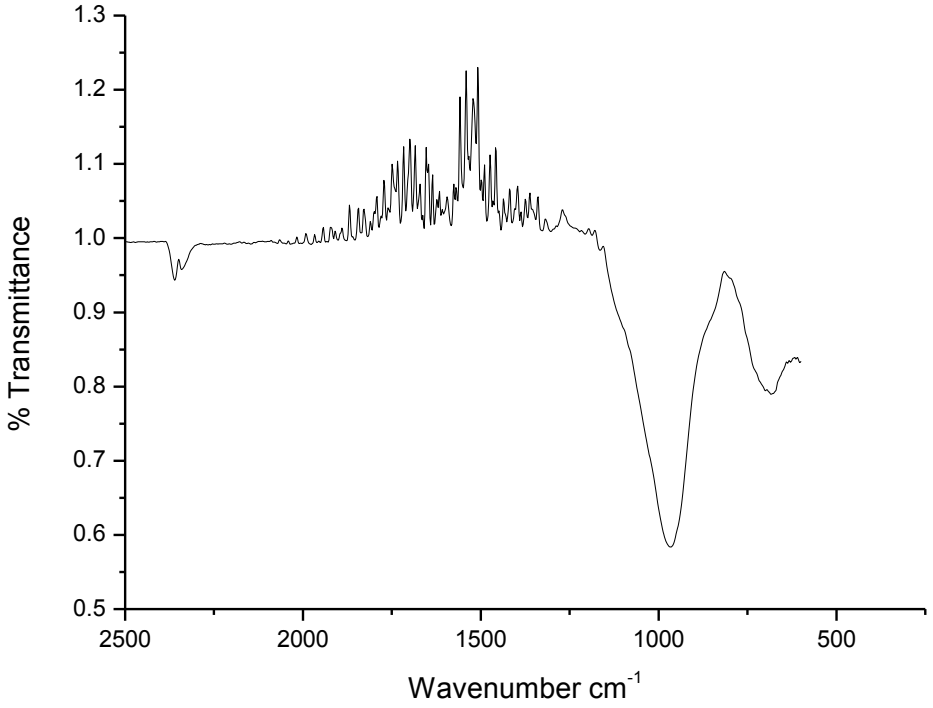

% Transmittance
1.3
1.2
1.1
1.0
0.9
0.8
0.7
0.6
0.5
2500
2000
1500
1000
500
Wavenumber cm-1

Figure 5

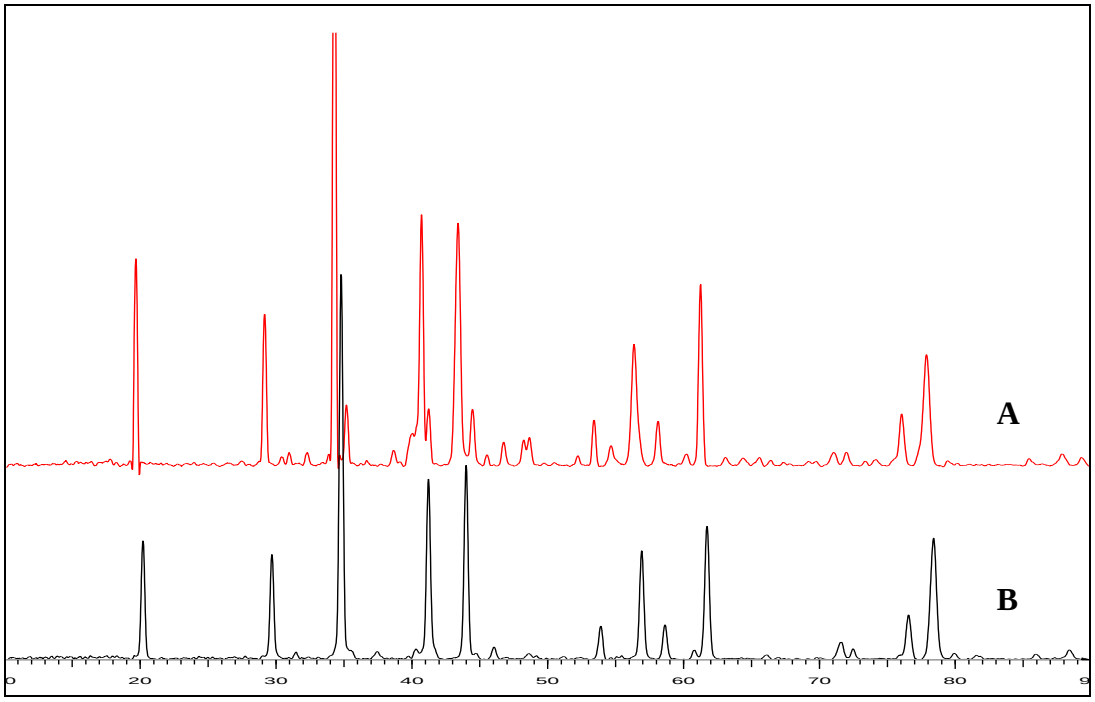


Figure 6.

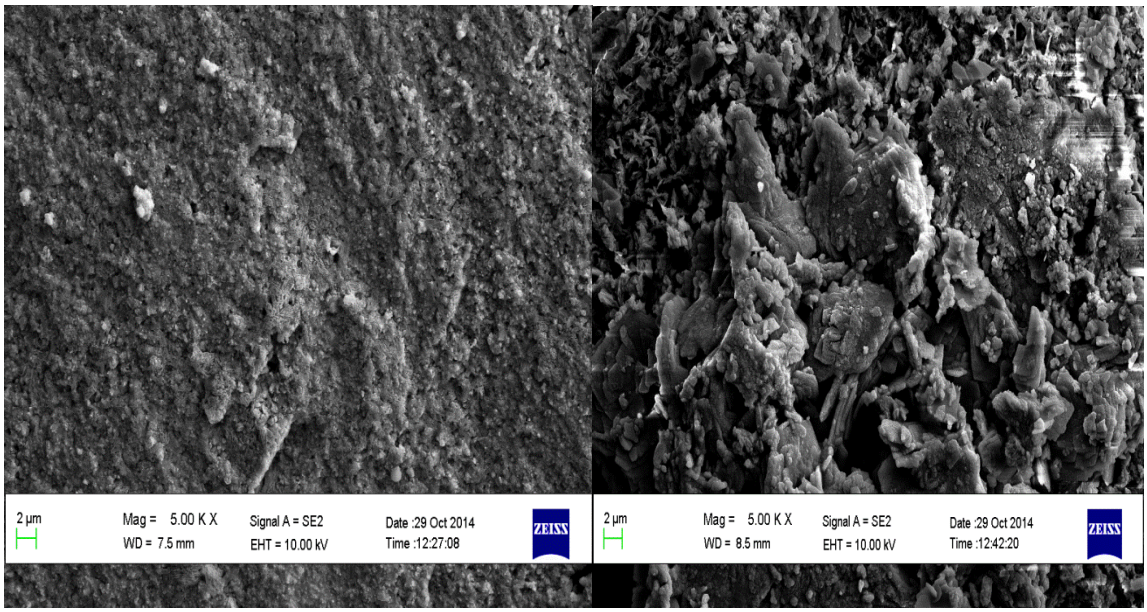

2 µm
Mag = 5.00 K X
WD = 7.5 mm
Signal A = SE2
EHT = 10.00 kV
Date :29 Oct 2014
Time :12:27:08
ZEISS
2 µm
Mag = 5.00 K X
WD = 8.5 mm
Signal A = SE2
EHT = 10.00 kV
Date :29 Oct 2014
Time :12:42:20
ZEISS

Figure 7

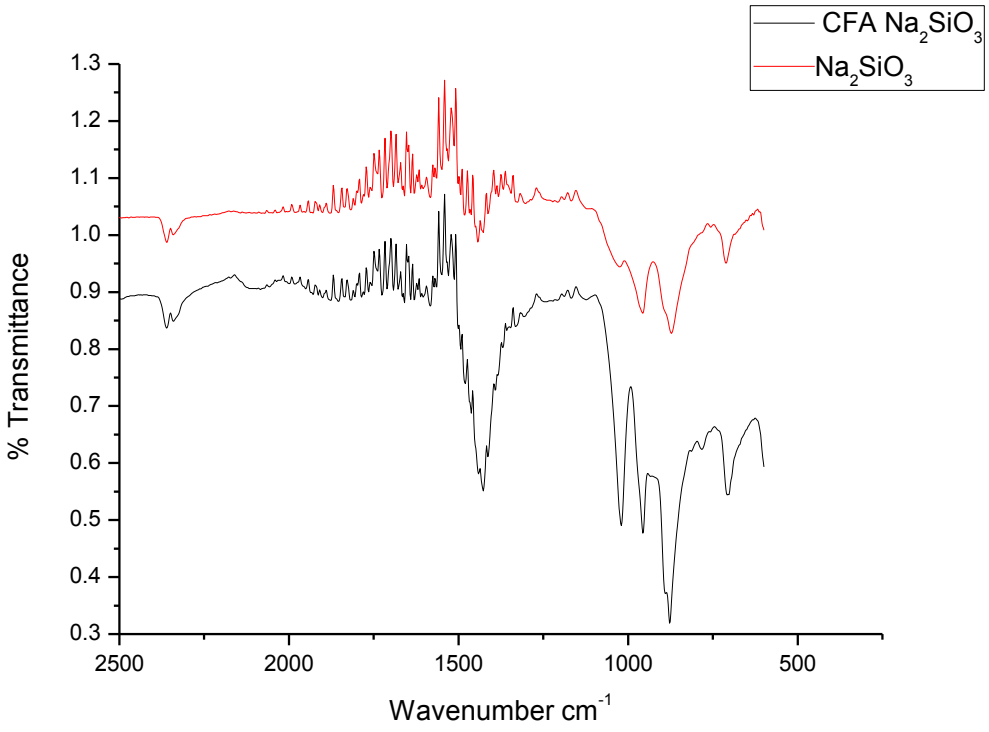

CFA Na_2SiO_3
Na_2SiO_3
% Transmittance
1.3
1.2
1.1
1.0
0.9
0.8
0.7
0.6
0.5
0.4
0.3
2500
2000
1500
1000
500
Wavenumber cm^{-1}

Figure 8

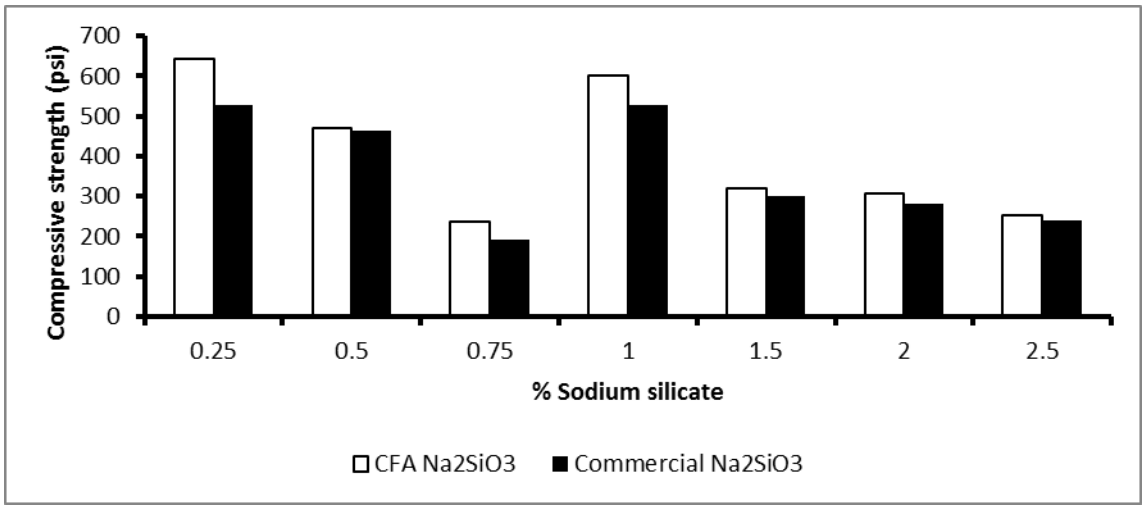

Compressive strength (psi)
700
600
500
400
300
200
100
0
0.25
0.5
0.75
1
1.5
2
2.5
% Sodium silicate
CFA Na2SiO3
Commercial Na2SiO3

Figure 9

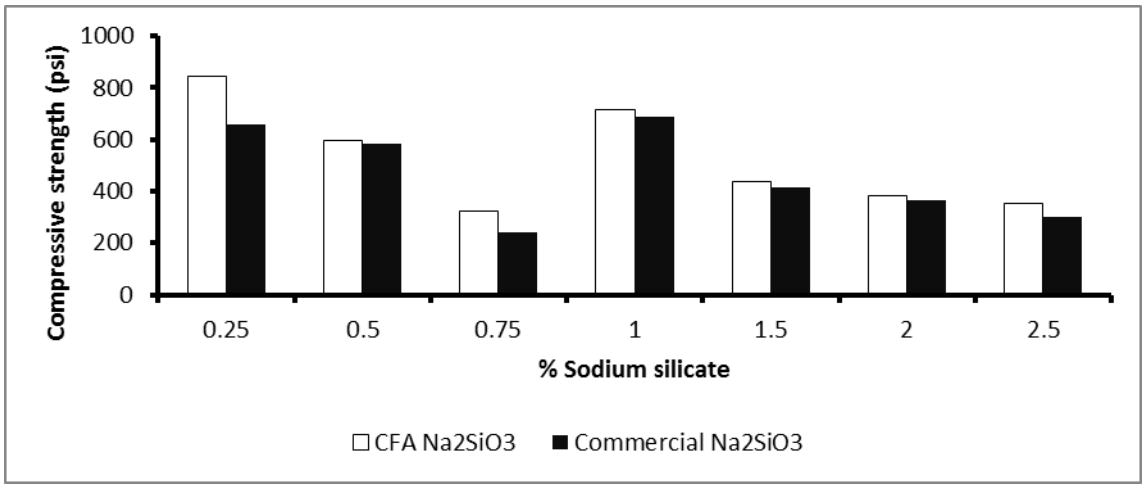

Compressive strength (psi)
1000
800
600
400
200
0
0.25
0.5
0.75
1
1.5
2
2.5
% Sodium silicate
CFA Na2SiO3
Commercial Na2SiO3

Figure 10

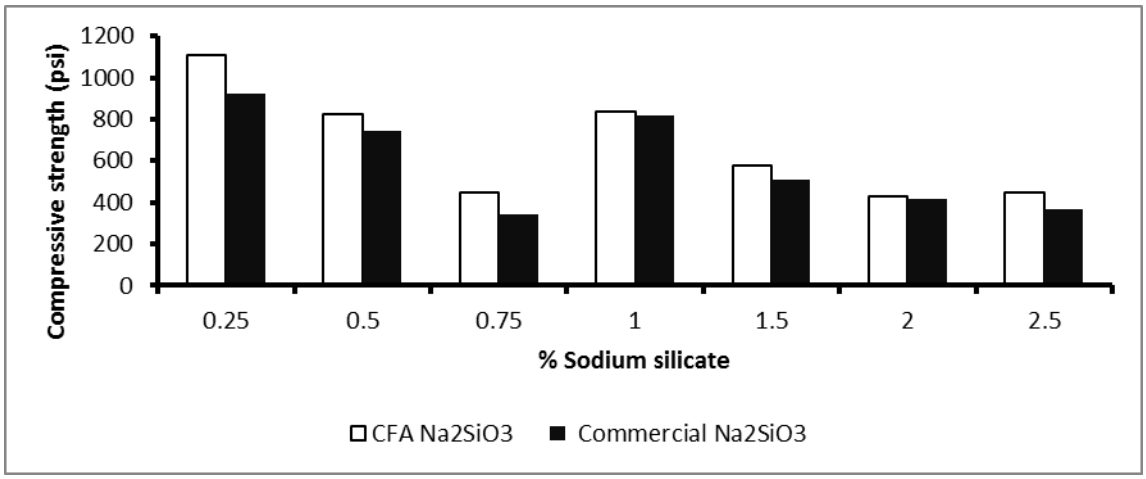

Compressive strength (psi)
1200
1000
800
600
400
200
0
0.25
0.5
0.75
1
1.5
2
2.5
% Sodium silicate
CFA Na2SiO3
Commercial Na2SiO3

Figure 11

Table

Table 1. XRF Results for Power Station X CFA (majors). Also included are XRF results for South African CFAs (Mainganye *et al.*, 2013and Ayanda *et al.*, 2012)

Table 2. Compositions and densities of the slurries

Table 3. Rheological properties of the slurries with com-Na_2SiO_3.

Table 4. Rheological properties of the slurries with CFA-Na_2SiO_3.

Table 5. UCA results for the slurries with com-Na_2SiO_3.

Table 6. UCA results for the slurries with CFA-Na_2SiO_3.

Table 1

Element	% Composition Power Station X CFA	Mainganye et al. 2013	Ayanda et al. 2012
SiO_2	57.9	55.66	51.43
Al_2O_3	31.12	27.95	30.93
Fe_2O_3	0.33	3.22	2.29
FeO	2.65	NR	NR
MnO	0.04	0.04	0.02
MgO	0.95	1.91	1.95
CaO	4.28	4.38	6.75
Na_2O	0.13	0.31	0.54
K_20	0.66	0.48	0.77
TiO_2	1.519	1.13	1.74
P_20_5	0.39	0.26	1.08
Cr_2O_3	0.0223	0.03	0.02
NiO	0.0008	NR	0.01
LOI	0.73	4.74	1.21
Sum %	**100.72**	**100.07**	**99.28**

Table 2

Sodium Silicate (%BWOC)	Water (%)	Class G Cement (g)	Slurry density (ppg) (Na_2SiO_3)	Slurry density (ppg) (CFA Na_2SiO_3)
0	44	792	15.8	15.8
0.25	68	677	14.0	14.0
0.5	78	638	13.4	13.5
0.75	104	555	12.5	12.4
1	78	637	13.5	13.4
1.5	80	627	13.1	13.0
2	88	595	13.0	12.8
2.5	100	556	12.8	12.6

Table 3

	% SS						
Rheology @ BHCT (rpm)	**0.25**	**0.5**	**0.75**	**1**	**1.5**	**2**	**2.5**
300	29	42.5	21.5	59	76	64	70
200	24.5	37	18.5	52	70.5	59	67.5
100	24	33	19	46.5	64	56	64.5
60	23	31.5	19	45	60	56	63
30	22	30	19.5	23.5	56	54	55.5
6	15	19	14	23	32	38.5	33
3	12	12	11.5	20	26	27	29.5
P_v (cp)	7.5	14.25	3.75	18.75	18	12	8.25
Y_p (lb/100ft^2)	21.5	28.25	17.75	40.25	58	52	61.75

Table 4

	%CFA SS						
Rheology @ BHCT (rpm)	**0.25**	**0.5**	**0.75**	**1**	**1.5**	**2**	**2.5**
300	31.5	43.5	24	37	31	44.5	40.5
200	24.5	38.5	19	33	25.5	40	36.5
100	19.5	36	18.5	26.5	24	37.5	33
60	17.5	32.5	19	26	23	36.5	31.5
30	15	31	17	27	21	36.5	31.5
6	8.5	17.5	14.5	15	16.5	22.5	22
3	10	8.5	12	11.5	10.5	19	17
P_v (cp)	18	11.25	8.25	15.75	10.5	10.5	11.25
Y_p (lb/100ft^2)	13.5	32.25	15.75	21.25	20.5	34	29.25

Table 5

	% SS						
UCA Results	**0.25**	**0.5**	**0.75**	**1**	**1.5**	**2**	**2.5**
50psi (hrs: min)	2:12:00	2:09:00	3:22:30	2:12:00	2:49:00	3:11:30	3:40:00
500psi (hrs: min)	7:26:00	8:58:00	_	7:41:00	22:47:00	_	_
8hrs Compressive Strength(psi)	527	465	191	529	301	281	241
12hrs Compressive Strength(psi)	658	583	243	689	416	367	298
24hrs Compressive Strength(psi)	920	741	345	820	512	419	364

Table 6

	% CFA SS						
UCA Results	**0.25**	**0.5**	**0.75**	**1**	**1.5**	**2**	**2.5**
50psi (hrs: min)	1:59:30	2:28:30	3:14:00	2:01:30	2:36:00	3:00:00	2:43:00
500psi (hrs: min)	5:41:00	8:45:30	_	7:37:30	21:43:30	_	_
8hrs Compressive Strength(psi)	643	471	236	601	319	307	253
12hrs Compressive Strength(psi)	842	597	321	714	439	381	351
24hrs Compressive Strength(psi)	1111	826	450	836	576	427	449